NUMERICAL ANALYSIS OF A REGULAR WAVE OVER A VERTICAL PILE WITH A SQUARE SECTION

Paulo Roberto de Freitas Teixeira, pauloteixeira@furg.br
Mateus das Neves Gomes, mateusufpel.gomes@gmail.com
Elizaldo Domingues dos Santos, elizaldosantos@furg.br
Liércio André Isoldi, liercioisoldi@furg.br
Luiz Alberto Oliveira Rocha, laorocha@gmail.com
Programa de Pós-Graduação em Modelagem Computacional (PPGMC) – Escola de Engenharia (EE) – Universidade Federal do Rio Grande (FURG) – Avenida Itália, km 8 – Rio Grande-RS

Abstract. *The study of the action of waves on piles is very important for the design of structures in coastal and oceanic areas. Currently, there is strong interest in analyzing the action of waves on piles with non-circular sections, such as rectangular or square ones. According to Vengatesan et al. (2000), the main reason for this interest is the low cost of the connections of the members in the structures with these sections. The objective of this paper is to analyze the action of a regular wave on a vertical pile with a square section employing two differents numerical methodologies for prediction of the wave fluid dynamic. To achieve this goal were used the FLUINCO and FLUENT® softwares. FLUINCO (Teixeira, 2001) employs a partitioned two-step semi-implicit Taylor-Galerkin method in the Navier-Stokes equations. The free surface is governed by its kinematic boundary condition and an arbitrary Lagrangian-Eulerian (ALE) formulation is used to enable movements of the free surface. The FLUENT® code (2006), version 6.3.26, implements a finite volume technique to solve the equation of continuity and the Navier-Stokes equations. The free surface is described by using the VOF method (Volume Of Fluid). The wave period of the studied problem is 4s and its height is 0.05 m. The pile is seated on the bottom and located in the center of a channel. The dimensions of the pile section are 1m × 1m and the channel is 30m long, 10m wide and 1m deep. This paper shows the results obtained by the models in terms of the velocity vectors, the deformation of the free surface and the drag force caused by the wave on the pile. The total horizontal force acting on the pile was analytically calculated using the Morison equation. It was observed very similar results to the numerical ones.*

Keywords*: Ocean waves, FLUINCO, FLUENT, Arbitrary Lagrangian-Eulerian (ALE), Volume of Fluid (VOF)*

1. INTRODUCTION

The study of the wave action over piles is very important for the design of structures in coastal and oceanic regions, for example in piers, pipelines and platforms. Several studies have examined the hydrodynamic loading over oceanic structures, especially piles with circular cross sectional area. Nowadays, there is much interest in analyzing the wave action over non circular piles, i.e., piles with rectangular or square cross sectional areas. In accordance with Vengatesan *et al.* (2000), the low cost of the connections among the parts of the structures is one of the reasons for this interest.

This case study consists of analyzing the action of an incident wave over a vertical pile with square cross sectional area. This problem was presented by Li and Lin (2001), who discussed the flow behavior around the pile. Moreover, the drag and inertial coefficients were calculated using a partitioned solution method for the Navier-Stokes equations (Li and Yu, 1996), the σ coordinate transformation and the subgrid scale (SGE) turbulence model. The σ coordinate is a dimensionless vertical coordinate employed when the algorithm needs a grid with the same number of layers throughout the domain, enabling a smooth vertical discretization in relation to the vertical z coordinate.

The aim of this paper is to analyze and to compare the results obtained by computational models FLUINCO (Teixeira, 2001) and FLUENT® (FLUENT, 2006) and those presented by Li and Lin (2001), considering the effects of an incident wave over a pile with a cross sectional area. Both numerical codes are based on the Navier-Stokes equations.

The FLUINCO model uses a partitioned two-step semi-implicit Taylor-Galerkin method for the temporal and spatial discretization of the Navier-Stokes equations (Teixeira, 2001). The free surface is mobile and governed by its kinematic boundary condition. The arbitrary lagrangian-eulerian formulation (ALE) enables the solution of problems involving large relative movements among bodies and surfaces as well as free surface movements. A model based on the Prandtl mixing length is applied to the turbulence modeling.

The commercial software FLUENT®, based on the Finite Volume Method (FVM), is a general computational fluid dynamic (CFD) package in which interaction between water and air on the free surface of a wave can be numerically represented, by applying the Volume of Fluid (VOF) method. The velocity components of the wave are used for generating the wave, and the turbulence was not considered.

2. NUMERICAL MODELS

2.1. FLUINCO

The algorithm is based on both mass and momentum conservation equations, and considers an ALE formulation (Teixeira and Awruch, 2000). It is described as follows:

(a) Calculate the non-corrected velocity at instant $t+\Delta t/2$ using the pressure term at time t, according to Eq. (1):

$$\tilde{U}_i^{n+1/2} = U_i^n - \frac{\Delta t}{2}\left(\frac{\partial f_{ij}^n}{\partial x_j} - \frac{\partial \tau_{ij}^n}{\partial x_j} + \frac{\partial p^n}{\partial x_i} - \rho g_i - w_j^n \frac{\partial U_i^n}{\partial x_i} \right) \quad (i, j = 1, 2, 3) \tag{1}$$

where p is the pressure, $U_i = \rho \mathrm{v}_i$, $f_{ij} = \mathrm{v}_j(\rho \mathrm{v}_i) = \mathrm{v}_j U_i$, ρ is the specific mass, v_i are the velocity components, w_i are the mesh velocity components, g_i are the gravity acceleration components, τ_{ij} are the components of deviatory tensor (i, j = 1, 2, 3).

(b) Update the pressure p at instant $t+\Delta t$, using the Poisson equation, given by:

$$\frac{1}{c^2}\Delta p = -\Delta t\left[\frac{\partial \tilde{U}_i^{n+1/2}}{\partial x_i} - \frac{\Delta t}{4}\frac{\partial}{\partial x_i}\frac{\partial \Delta p}{\partial x_i} \right] \quad (i = 1, 2, 3) \tag{2}$$

where $\Delta p = p^{n+1} - p^n$.

(c) Update the velocity at $t+\Delta t/2$, adding the pressure variation term from instant t to $t+\Delta t/2$, in the expression:

$$U_i^{n+1/2} = \tilde{U}_i^{n+1/2} - \frac{\Delta t}{4}\frac{\partial \Delta p}{\partial x_i} \quad (i, j = 1, 2, 3) \tag{3}$$

(d) Calculate the velocity at $t+\Delta t$ using the variables updated in the previous steps, as follows:

$$U_i^{n+1} = U_i^n - \Delta t\left(\frac{\partial f_{ij}^{n+1/2}}{\partial x_j} - \frac{\partial \tau_{ij}^{n+1/2}}{\partial x_j} + \frac{\partial p^{n+1/2}}{\partial x_i} - w_j^{n+1/2}\frac{\partial U_i^{n+1/2}}{\partial x_i} - \rho g_i \right) \quad (i, j = 1, 2, 3) \tag{4}$$

The classical Galerkin weighted residual method is applied to the space discretization by using tetrahedral elements. In the variables at instant $t+\Delta t/2$, a constant shape function is used, and in the variables at t and $t+\Delta t$, a linear shape function is employed.

The free surface is the interface between two fluids, water and air, and the atmospheric pressure is considered constant (generally, the reference value is null). In this interface, the Kinematic free surface boundary condition (KFSBC) is imposed. By using the ALE formulation, it is expressed as (Ramaswamy and Kawahara, 1987):

$$\frac{\partial \eta}{\partial t} + \left({}^{(s)}\mathrm{v}_i - {}^{(s)}\mathrm{w}_i \right)\frac{\partial \eta}{\partial x_i} = 0 \quad (i = 1, 2, 3) \tag{5}$$

where η is the free surface elevation, ${}^{(s)}\mathrm{v}_i$ and ${}^{(s)}\mathrm{w}_i$ are the fluid and mesh velocity components in the free surface, respectively. The eulerian formulation is used in the x and y directions (horizontal plane) while the ALE formulation is employed in the z or vertical direction. The time discretization of KFSBC is carried out in the same way as the one for the momentum equations, previously presented. Triangular elements coincident with tetrahedral faces of the free surface are adopted to space discretization.

The mesh velocity vertical component w_3 is computed to diminish element distortions, keeping prescribed velocities on moving (free surface) and stationary (bottom) boundary surfaces. The mesh movement algorithm uses a smoothing procedure for the velocities based on these boundary surfaces. The updating of the mesh velocity at point i of the finite element domain is based on the mesh velocity of the points j that belong to the boundary surfaces.

The elevation and the velocity components of the linear wave theory (Dean and Dalrymple, 1994) are imposed directly on the wave generation boundary condition. The radiation condition, similar to Flather's proposal (1976), is imposed on open boundaries.

An eddy viscosity approach is used for turbulence modeling. The Reynolds stresses are modeled using a generalization of the Prandtl mixing length hypothesis. This model was also employed by Mittal and Tezduyar (1995), and consists of the addition of an eddy viscosity, ν_t, to the molecular kinematic viscosity, ν. The eddy viscosity is given by the following expression:

$$\nu_t = (k\,lm)^2 \sqrt{2(S_{ij}S_{ij})} \quad (i,j=1,2,3) \tag{6}$$

where k=0.41 is the von Kármán constant, S_{ij} is a tensor given by:

$$S_{ij} = \frac{1}{2}\left(\frac{\partial v_i}{\partial x_j} + \frac{\partial v_j}{\partial x_i}\right) \quad (i,j=1,2,3) \tag{7}$$

and lm is the mixed length that, according to Johns (1991), is written as:

$$lm = \frac{(z+h+z_0)(\eta - z + z_s)}{h+\eta+z_0+z_s} \quad (i,j=1,2,3) \tag{8}$$

where z_0 and z_s are roughness length of bottom and free surfaces, respectively, and h is the depth.

2.2. FLUENT

The FLUENT® software is a Computational Fluid Dynamics (CFD) package used for modeling fluid flow and heat transfer in complex geometries. It is based on the Finite-Volume Method (FVM) to solve the governing equations of the problem.

The Volume of Fluid (VOF) model was adopted for wave generation in the FLUENT® code. The VOF model is a surface-tracking technique applied to a fixed Eulerian mesh. It is designed for two or more immiscible fluids, where the position of the interface between the fluids is of interest. In this study, the two fluids are water and air.

In the VOF model, a single set of momentum equations is shared by the fluids (FLUENT, 2006):

$$\frac{\partial}{\partial t}(\rho\vec{v}) + \nabla\cdot(\rho\vec{v}\vec{v}) = -\nabla p + \nabla\cdot\left[\mu\left(\nabla\vec{v} + \nabla\vec{v}^T\right)\right] + \rho\vec{g} + \vec{F} \tag{9}$$

and the volume fraction of each fluid in each computational cell is tracked throughout the domain:

$$\frac{1}{\rho_q}\left[\frac{\partial}{\partial t}(\alpha_q\rho_q) + \nabla(\alpha_q\rho_q\vec{v}_q) = S_{\alpha_q} + \sum_{p=1}^{n}(\dot{m}_{pq} - \dot{m}_{qp})\right] \tag{10}$$

where t is the time, ρ is the specific mass, $\vec{v}$ is the velocity vector, p is the static pressure, μ is the viscosity, $\rho\vec{g}$ is the gravitational force, $\vec{F}$ are the external forces, α_q is the q^{th} fluid volume fraction in the cell, S_{α_q} is the source term, $\dot{m}_{pq}$ is the mass transfer from phase p to phase q and $\dot{m}_{qp}$ is the mass transfer from phase q to phase p.

3. DESCRIPTION OF THE PROBLEM

The geometry employed in this study is depicted in Fig. 1. A three-dimensional channel with the following dimensions: L = 30 m (length), W = 10 m (width), h = 1 m (deep of water layer) and h_1 = 1.2 m is analyzed. The channel height, h_1, is just employed for the simulations in which the free surface flows are approached by the VOF methodology, i.e., for the simulations performed by FLUENT®; in the other cases, the channel height is h. A square cross section pile of dimension D = 1 m is placed at distance L_1 = 10 m from the channel inlet (Fig. 1). For the simulation with FLUINCO code, the working fluid employed is water, with specific mass ρ = 1000.0 kg/m³ and dynamical viscosity μ = 0.001 Ns/m^2. Flows with water-air mixture are used for simulations with FLUENT®. It is worth mentioning that VOF formulation is based on the hypothesis of two or more impenetrable phases since the rate of the density between water and air is much higher than unity. A wave period T = 4 s (frequency ω = 1.5708 Hz) and height H_w = 0.05 m is imposed in the inlet boundary condition. From the dispersion equation, based on the linear theory (Dean and Dalrymple, 1994), the wavelength is calculated; it corresponds to L_W = 12.0 m (wavenumber k = 0.5236 m^{-1}).

The case study presents wave steepness 0.0031 m/s², defined by H_w/T^2, relative depth 0.0625 m/s², defined by h/T^2 and an Ursell number Ur = 3.6 (L^2H_w/h^3). These parameters suggest that the behavior of the wave is found in the transition between the linear theory and the second order Stokes theory (Chakrabarti, 1994). The Keulegan-Carpenter parameter is KC = 0.33 ($u_m T/D$), where u_m = 0,0817m/s is the particle maximum horizontal velocity and D = 1 m is the dimension of the pile edge. In lower KC values, such as the ones found in this case, the fluid particles never cross the structure during a period of the wave. Besides, the effects concerned the drag can be neglected in comparison with the inertial ones. The diffraction parameter found in this case is 0.26 ($\pi D/L$), suggesting that diffraction has little significance.

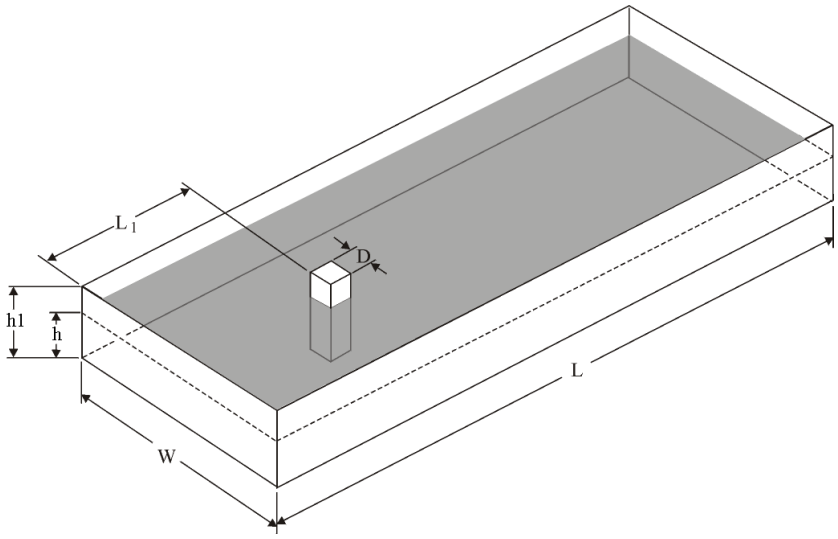

Figure 1. Computational domain of the problem under analysis.

In order to reduce the computational effort, the simulations are performed in half of the domain, adopting the symmetry condition at $y = W/2$. For the simulations of laminar flows, some three-dimensional effects can be neglected, reinforcing the hypothesis employed in this paper.

For the simulations with the FLUINCO code, the finite element method with a mesh of 201900 tetrahedral elements and 46266 nodes is used. This mesh represents 10 divisions in the vertical direction, 130 divisions in the length of the channel and 33 divisions in the width dimension. The mesh employed in this study is stretched with a higher refinement near the pile. The lowest element dimension near the pile is 60 mm. For the inlet boundary condition, the surface elevation is imposed, as well as the velocity field for a linear. The radiation boundary condition for the outlet surface is also imposed. For the lateral surfaces of the channel, as well as the pile surfaces, the non-slip condition is employed. Concerning the initial boundary conditions, the hydrostatic pressure is employed, while the velocity and the surface elevation are at rest. The time step Δt = 0.003 s is used and the simulation is performed until t = 40 s.

A regular mesh with 1435200 hexahedral finite volumes is used for the simulations performed by the FLUENT® package. This regular mesh is constructed with an interval size 0.05 m. On the top of the channel, the pressure outlet is the atmospheric pressure; in the walls (the bottom and lateral surfaces of the channel and the pile surfaces), the non-slip condition is applied; and in the inlet boundary condition, a User Defined Function (UDF) is employed by using the velocity components of the wave:

$$u = Agk\frac{\cosh(kz+kh)}{\omega\cosh(kh)}\cos(kx-\omega t) + A^2\omega k\frac{\cosh 2k(k+z)}{sen^4(kh)}\cos 2(kx-\omega t) \tag{11}$$

$$w = Agk\frac{sinh(kz+kh)}{\omega sinh(kh)}sin(kx-\omega t) + A^2\omega k\frac{sinh 2k(k+z)}{\cos^4(kh)}sin 2(kx-\omega t) \tag{12}$$

where A is the wave amplitude, g is the acceleration due to gravity, k is the wave number (given by $k = 2\pi/L$, being L the wavelength), h is the water depth, ω is the frequency (given by $\omega = 2\pi/T$, being T the wave period), x is the position, t is the time and z is the position variation between the free surface and the bottom.

4. RESULTS AND DISCUSSIONS

The profiles of the free surface along the symmetrical plane are shown in Fig. 2. It can be seen that the pile is placed in the range $-0.5 \leq x \leq 0.5$. Five free surface profiles during a wave period are shown; they correspond to the following instants: 28s ($t/T = 7.0$), 28.8s ($t/T = 7.2$), 29.6s ($t/T = 7.4$), 30.4s ($t/T = 7.6$), 31.2s ($t/T = 7.8$) and 32s ($t/T = 8.0$), which can be seen in Fig. 2a - 2f, respectively. The results obtained by FLUENT are compared with the previous ones obtained by FLUINCO and found by Li and Lin (2001). In general, the results have a similar behavior. However, during the wave propagation around the obstacle, some discrepancies due to the influence of the pile are observed. This fact causes quite a difference between the water elevation downstream and upstream. It is also noticed that, in general, the results achieved by the FLUENT code are less damped than the ones predicted by the FLUINCO code, except for $t/T = 8$, Fig. 2f, where the wave obtained by the FLUENT simulations is significantly more damped than the one presented by Li and Lin (2001) and FLUINCO. Perhaps this fact is concerned with the beginning of the wave reflection due to the influence of the outlet channel surface. Moreover, the results presented by Li and Lin (2001) seem unaffected by the presence of the pile. They are neither shown in FLUINCO simulations nor in predictions presented by FLUENT.

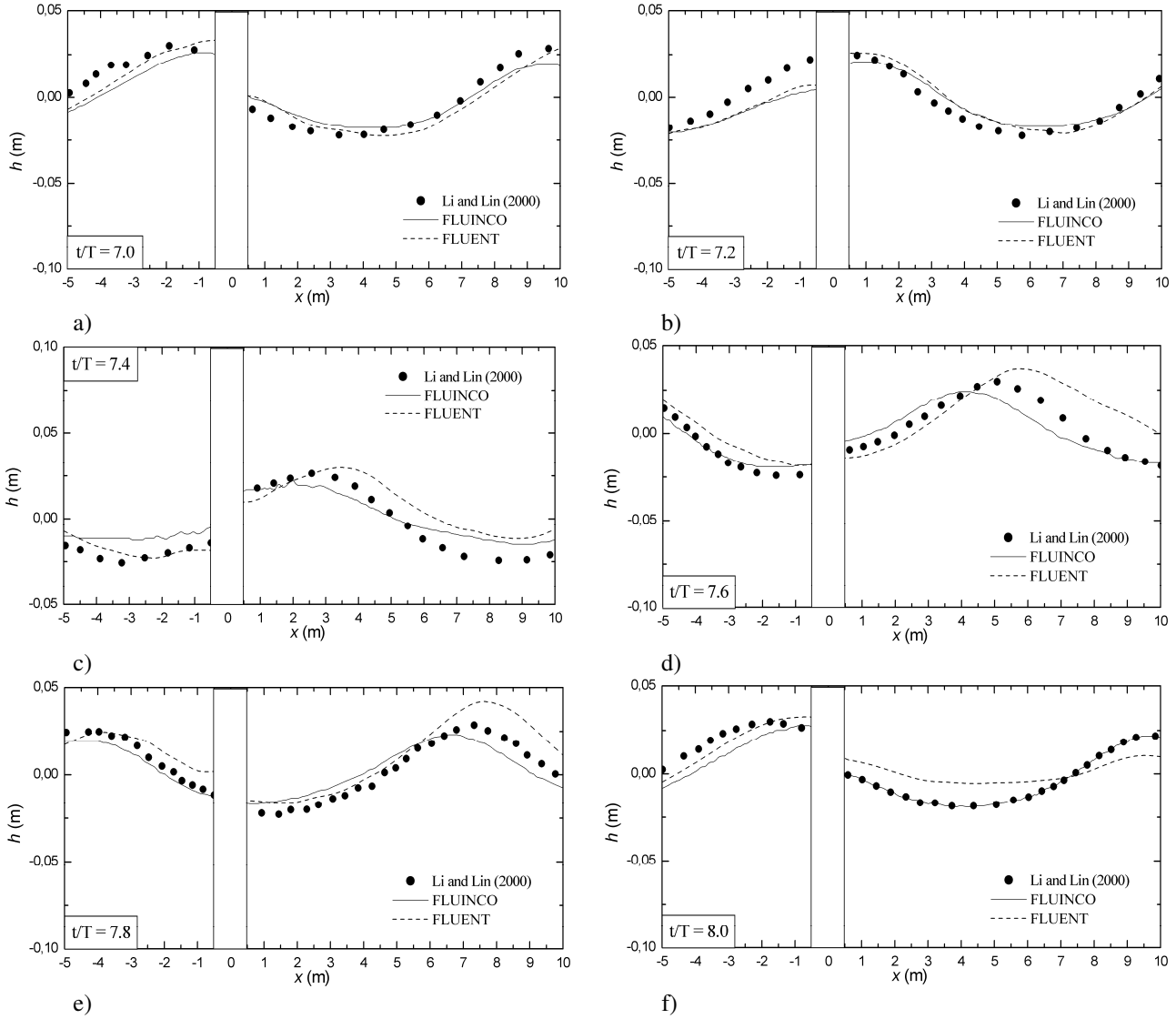

Figure 2. Free surface wave profiles for the following rates between time and wave period: (a) $t/T = 7.0$, (b) $t/T = 7.2$, (c) $t/T = 7.4$, (d) $t/T = 7.6$, (e) $t/T = 7.8$ and (f) $t/T = 8.0$.

Figure 3 shows the distribution of the velocity vectors in a region near the pile predicted by the FLUINCO and FLUENT codes. These distributions are obtained for a horizontal section plane at 0.5m depth. One period of the wave propagation at the same instants previously presented for the profiles of the free surface is represented: 28.0s ($t/T = 7.0$), 28.8s ($t/T = 7.2$), 29.6s ($t/T = 7.4$), 30.4s ($t/T = 7.6$), 31.2s ($t/T = 7.8$) and 32.0s ($t/T = 8.0$). These instants are represented by Fig. 3a, 3c, 3e, 3g, 3i and 3l, respectively, for the simulations performed by FLUINCO and Fig. 3b, 3d,

3f, 3h and 3m, respectively, for the simulations carried out by FLUENT. As previously observed in the results of the free surface profiles, the predictions performed by the FLUINCO and the FLUENT codes have similar behavior. Both simulations show that the velocity vectors have the same direction of the wave propagation around the crest, while in the trough, the opposite effect is noticed. The presence of vortices in the four corners of the pile is also observed. It is worth mentioning that the vortices are suppressed near the pile structure, probably due to the oscillating behavior of the wave which inhibits the vortex shedding. This behavior is quite different from the one noticed when the obstacle is surrounded by a uniform flow. The latter usually shows vortex shedding, even for flows at laminar regime (Li and Lin, 2001).

In this case, the presence of the pile weakly influences the wave diffraction effects, since the diffraction parameter is considered low. Besides, diagrams related with the application field of the wave-structure theories (Chakrabarti, 1994) show that, in this case, the calculus of the wave-structure forces can be performed by the use of the Morison equation. This equation assumes that the action forces over the pile is a linear composition of the inertial and viscous (drag) forces. The Morison equation, which was developed initially for a pile with circular cross section, is given by:

$$f = C_M A_I \frac{\partial u}{\partial t} + C_D A_D |u| u \,, \tag{13}$$

where f is the force per length (N/m); C_M and C_D are the inertial and viscous coefficients, respectively; u is the instantaneous velocity of the particle (m/s); ρ is the specific mass of the fluid (kg/m³), D is the cylinder diameter (m); $A_D = \rho D/2$ and $A_I = \rho \pi D^2/4$.

The original Morison equation has been developed for several applications, including tilted structures (Borgman, 1958), oscillating structures (Sarpkaya, 1976) and chains over the influence of waves (Moe and Verley, 1980). In this case study, Li and Lin (2001) proposed the following drag and inertial coefficients: $C_D = 1{,}0633$ and $C_M = 2{,}2662$, respectively. The total force (F_x), which acts over the pile, can be obtained by the integration of Eq. (13) along the depth of the pile and is written by (Chakrabarti, 1994):

$$F_x = \rho g V \left(\frac{H}{2h}\right) \tanh kh \left[C_M \operatorname{sen}(kx - \omega t) + C_D \left(\frac{H}{8D}\right) \frac{2kh + \operatorname{sen} 2kh}{\operatorname{senh}^2 kh} |\cos(kx - \omega t)| \cos(kx - \omega t) \right] \tag{14}$$

where V is the submerged portion volume of the pile (m³). The inertial and viscous forces are represented by the first and second terms of Eq. (14), respectively. In this case, Eq. (14) can be rewritten by:

$$F_x = 267.0 \ \operatorname{sen}(kx - \omega t) + 6.0 |\cos(kx - \omega t)| \cos(kx - \omega t) \quad [\mathrm{N}]. \tag{15}$$

It is possible to observe that the second term of Eq. (15), concerned with the drag, has a significantly lower magnitude in comparison with the inertial composition of the force. This fact explains why the incident force over the pile is 90 degrees lagged in comparison with the wave free-surface elevation. Figure 4 presents drag and inertia forces as a function of the time for this problem.

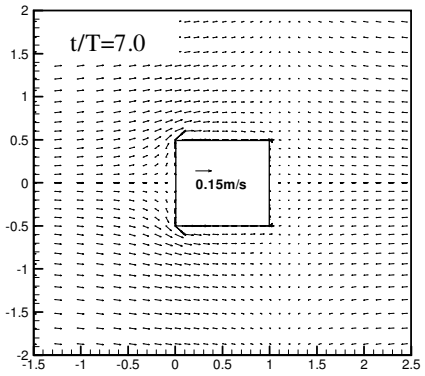

a)

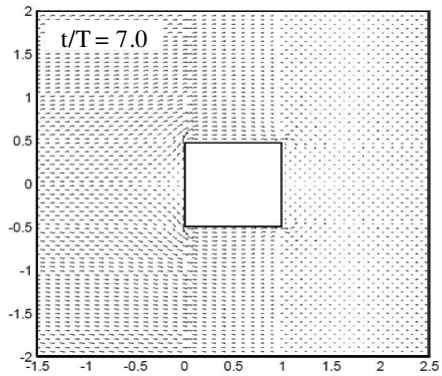

b)

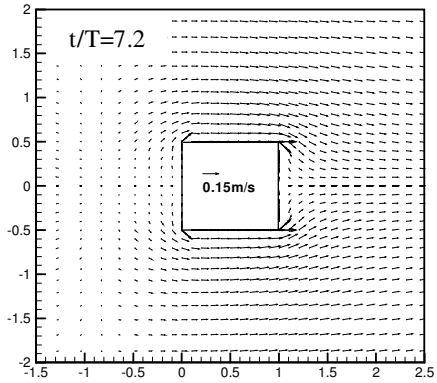
t/T=7.2
0.15m/s

c)

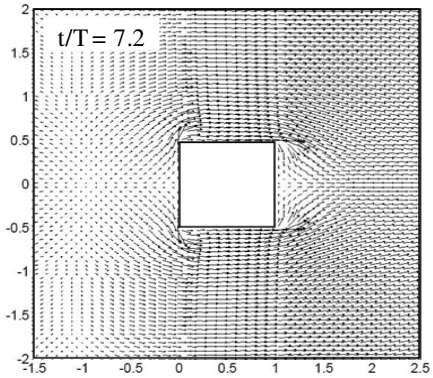
t/T = 7.2

d)

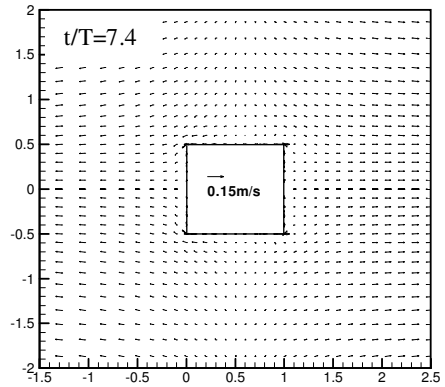
t/T=7.4
0.15m/s

e)

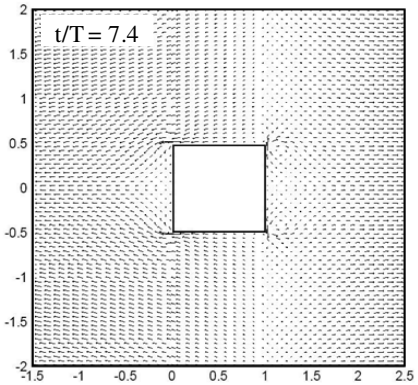
t/T = 7.4

f)

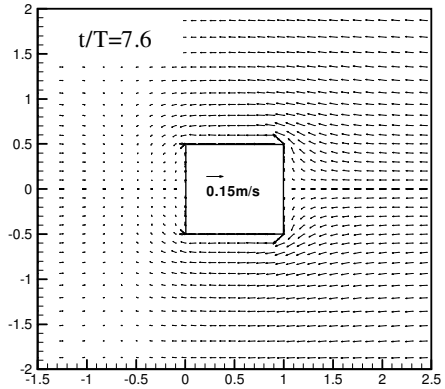
t/T=7.6
0.15m/s

g)

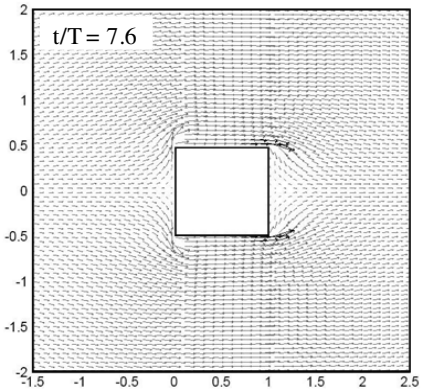
t/T = 7.6

h)

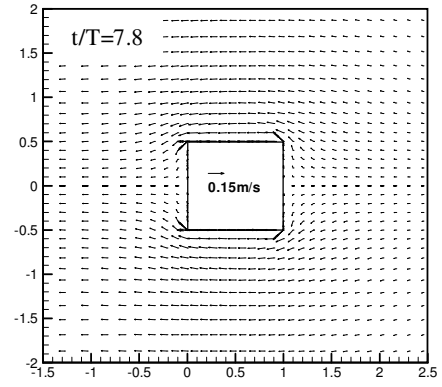
t/T=7.8
0.15m/s

i)

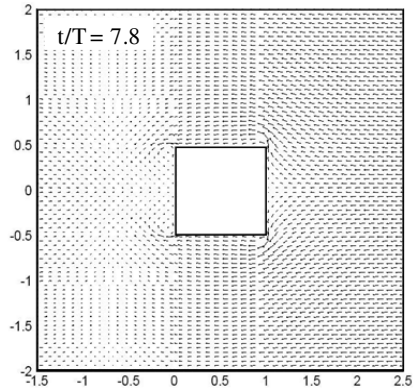
t/T = 7.8

j)

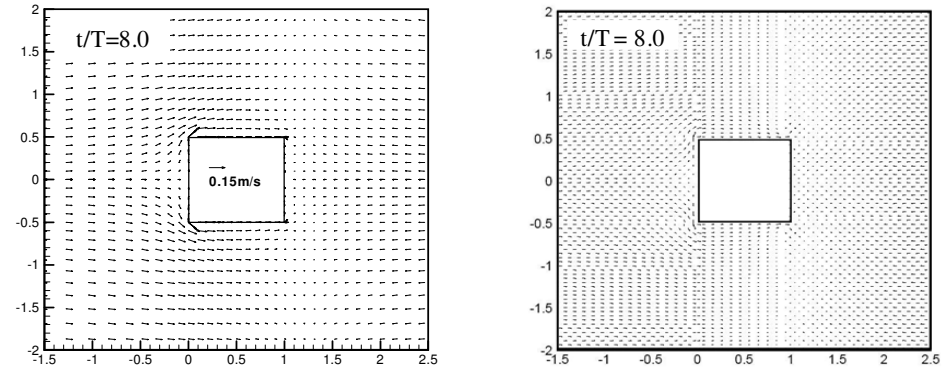

l) m)

Figure 3. The distribution of the velocity vectors during a wave period obtained by FLUINCO code (left) and by FLUENT code (right) for the following instants: (a), (b) $t/T = 7.0$; (c), (d) $t/T = 7.2$; (e), (f) $t/T = 7.4$; (g), (h) $t/T = 7.6$; (i), (j) $t/T = 7.8$; (l), (m) $t/T = 8.0$

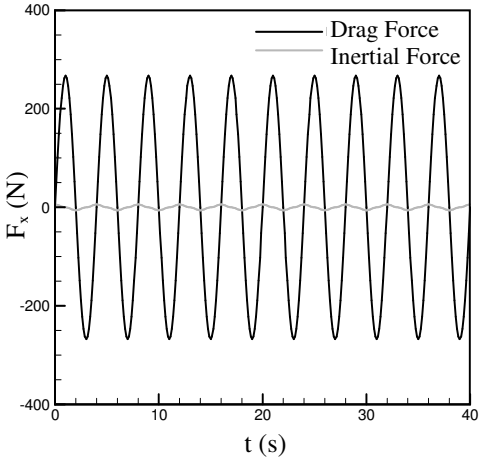

Figure 4. Drag and inertial forces over the pile predicted by the Morison equation

In the numerical simulations, the total force was calculated by the integration of pressure in the areas whose orthonormal vector is parallel to the direction of wave propagation. According to Li and Lin (2001), the viscous forces can be neglected, since their magnitude is approximately two orders lower than those reached by the pressure forces. Therefore, the same simplified hypothesis is used in this study. Figure 5 presents the total force in the wave propagation direction, F_x, as a function of time for the predictions obtained by FLUINCO and FLUENT. The results achieved with the numerical simulations are also compared with the total force calculated by the Morison equation. Both numerical codes, FLUENT and FLUINCO, agreed very well with the results obtained by the Morison equation.

5. CONCLUSIONS

This paper presented a numerical analysis of the incidence of a monochromatic wave over a square cross section pile. The FLUINCO (Teixeira, 2001) and FLUENT (FLUENT, 2006) codes were employed. The FLUINCO code is based on the finite element method with linear tetrahedral element. This code uses a partitioned method of the primary variables and correction for the velocity field. The temporal discretization is performed by a two-step semi-implicit Taylor-Galerkin scheme. This algorithm employs the ALE formulation to follow the free-surface movements. The FLUENT code is a CFD package based on rectangular finite volume. The solver is pressure based, the pressure coupling is performed by the SIMPLE method and for the treatment of advective dominant flows, the Upwind scheme is employed.

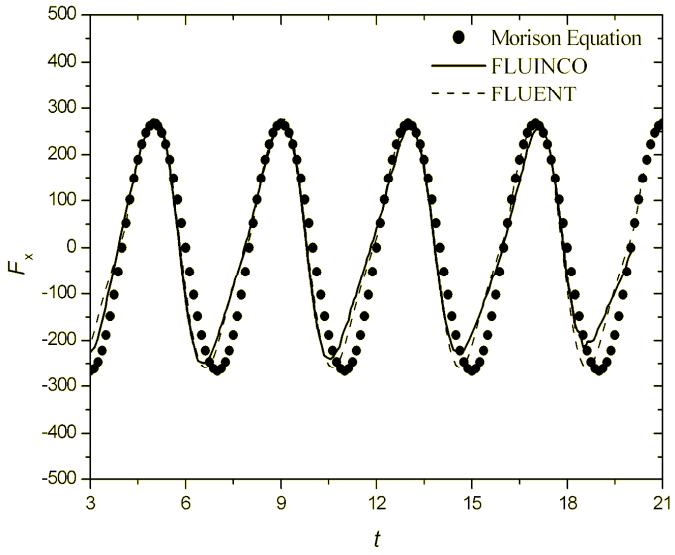

Figure 5. A comparison of the total force (F_x) over the pile as a function of time obtained by FLUINCO, FLUENT and predicted by the Morison equation.

The results include the flow and free surface characteristics of a flow over a pile, which is placed inside a wave channel. These results were compared with the results presented by Li and Lin (2001). In general, the fluid dynamic behavior of the free surface in the region near the pile predicted by both numerical codes was similar to the previous results presented by these authors. It was also observed that the free surfaces as a function of time achieved by FLUINCO and FLUENT had a good agreement with the Li and Lin's results. The total horizontal force (F_x) which acts over the pile as a function of time was also obtained. This force (F_x) was calculated analytically by using the Morison equation. It was noticed that the drag forces can be neglected in comparison with the inertial forces. This force was also numerically obtained by the FLUINCO and FLUENT codes, and a close agreement among the numerical and analytical predictions was observed.

This case study has shown the ability of the numerical codes, FLUINCO and FLUENT, to represent problems concerned with the interaction among wave and three-dimensional structures appropriately.

6. REFERENCES

Borgman, L. E., 1958, "Computation of the ocean-wave forces on inclined cylinders", Journal of Geophysical Research, Transactions AGU, Vol. 39, No. 5, pp. 885-888.

Chakrabarti, S. K., 1994, "Hydrodynamics of Offshore Structures", Computational Mechanics Publications.

Dean, R.G., Dalrymple, R.A., 1994, "Water Wave Mechanics for Engineers and Scientists", In: Advanced Series on Ocean Engineering**,** Vol. 2, World Scientific Publishing Co. Ltd.

Fluent, ANSYS, Inc., 2006.

Flather, R.A., 1976, "A tidal model of the northwest European continental shelf", Mem. Soc. R. Liege, Vol. 6, No. 10, pp. 141-164.

Johns, B., 1991, "The modeling of the free surface flow of water over topography", Coastal Eng., Vol.15, pp. 257-278.

Li, C.W. and Yu, T.S., 1996, "Numerical investigation of turbulent shallow recirculating flows by a quasi-three-dimensional $k-\varepsilon$ model", Int. J. Num. Met. Fluids, Vol. 23, pp. 485-501.

Li, C.W. and Lin, P., 2001, "A numerical study of three-dimensional wave interaction with a square cylinder", Ocean Enginieering, Vol. 28, pp. 1545-1555.

Mittal, S., Tezduyar, T.E., 1995, "Parallel finite element simulation of 3D incompressible flows-fluid-structure interaction", Int. J. Num. Meth. Fluids, Vol. 21, pp. 933–953.

Moe, G., Verley, R.L.P., 1980, "Hydrodynamic damping of offshore structures in wave currents", Proceedings of the Twelfth Offshore Technology Conference, Houston, Texas, OTC 3798, pp. 37-44.

Ramaswamy, R., Kawahara , M., 1987, "Arbitrary lagrangian-eulerian finite element method for unsteady, convective, incompressible viscous free surface fluid flow", International Journal for Numerical Methods in Fluids, Vol. 7, pp. 1053-1075.

Sarpkaya, T., 1976, "Vortex Shedding and Resistance in Harmonic Flow about Smooth and Rough Circular Cylinders at High Reynolds Numbers", Rep. NPS-59SL76021, U.S. Naval Postgraduate School.

Teixeira, P.R.F., 2001, "Simulação numérica da interação de escoamentos tridimensionais de fluídos compressíveis e incompressíveis e estruturas deformáveis usando o método de elementos finitos", Tese de doutorado, PPGEC-UFRGS, Porto Alegre.

Teixeira, P.R.F., Awruch, A.M., 2000, "Numerical simulation of three dimensional incompressible flows using the finite element method", *ENCIT*, 8, Porto Alegre.

Vengatesan, V., Varyani, K.S., Barltrop, N.D.P., 2000, "Wave-current forces on rectangular cylinder at low KC numbers", International Journal of Offshore and Polar Engineering, Vol. 10, N. 4, pp. 276-284.

7. RESPONSIBILITY NOTICE

The authors are the only responsible for the printed material included in this paper.